

FLAT BEAM PWFA THEORY AND EXPERIMENT AT AWA

P. Manwani*, Y. Kang, J. Mann, G. Andonian, B. Naranjo, J. B. Rosenzweig

UCLA, Los Angeles, CA, USA

A. Ody, P. Piot, D. Scott, E. Wisniewski, W. Liu, J. Power

Argonne National Laboratory, Lemont, IL, USA

N. Majernik, SLAC National Accelerator Laboratory, Menlo Park, CA, USA

K. Huang, Kansai Institute for Photon Science, Kizugawa-city, Kyoto, Japan

Abstract

In plasma wakefield acceleration, when the driver beam is denser than the plasma, there is an expulsion of the plasma electrons from the beam channel, resulting in an ion filled cavity. This cavity is called a bubble and has been well studied for round beams which result in an axisymmetric bubble. However, transversely asymmetric (flat) beams create elliptical bubbles, which have key differences. They offer asymmetric but linear focusing, with non-uniform acceleration, which is distinct from the axisymmetric case. We discuss the theory on beam-plasma interaction and present an experimental study in the context of the Argonne Wakefield Accelerator (AWA) which has capabilities for flat beams.

INTRODUCTION

Particle beams with asymmetric transverse emittances and profiles can be used to drive asymmetric plasma wakefields. The axisymmetric blowout regime has been extensively studied in the context of plasma wakefield acceleration [1–3]. Here, we discuss the formalism for the elliptical blowout created by the beam and show that the focusing forces that are transversely asymmetric. We utilize the ellipticity of the plasma ion cavity to model the beam evolution of the flat beam driver in a plasma capillary (developed at UCLA) [4], in preparation for the flat beam plasma wakefield acceleration (PWFA) experiment at the AWA. [5, 6].

FLAT BEAM PWFA INTERACTION

The theory of elliptical blowouts, created when the flat beam driver is denser than the plasma density, has been documented in detail in Ref. [7], which shows that the transverse wakefields are linear and depend on the semi major (a_p) and minor axes (b_p) of the transverse ellipse. We can write down the transverse wakefields as

$$\begin{aligned} W_x &= E_x - B_y = x \left(\frac{b_p^2}{a_p^2 + b_p^2} \right) = x \left(\frac{1}{\alpha_p^2 + 1} \right) \\ W_y &= E_y + B_x = y \left(\frac{a_p^2}{a_p^2 + b_p^2} \right) = y \left(\frac{\alpha_p^2}{\alpha_p^2 + 1} \right). \end{aligned} \quad (1)$$

Here we define $\alpha_p = a_p/b_p$ as the ellipticity of the blowout, where a_p and b_p are the semi-major and semi-minor axes of the ion cavity, respectively. In contrast to the axisymmetric

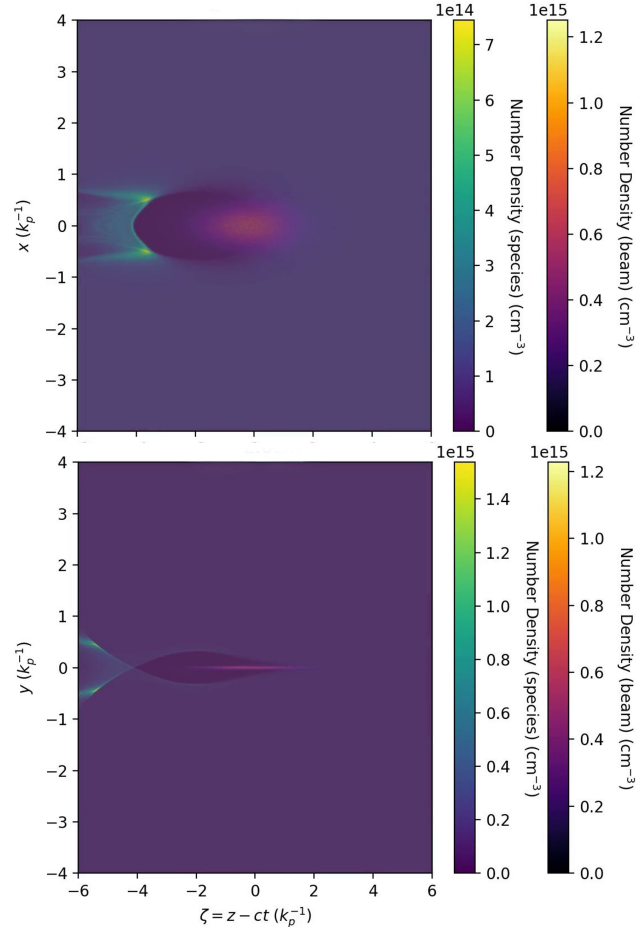


Figure 1: Asymmetric plasma blowout created by the flat beam driver, using the parameters in Table 1.

case ($\alpha_p = 1$), the transverse focusing forces differ in the x and y directions, resulting in distinct betatron wavenumbers in each plane. This asymmetry modifies the beam-matching conditions that are needed for emittance preservation [8], requiring that the beam sizes and divergences be adjusted in the two transverse directions to maintain matched propagation through the plasma. The new matched beta functions are

$$\beta_x = \sqrt{(1 + \alpha_p^2)\gamma} k_p^{-1} \quad (2)$$

$$\beta_y = \sqrt{\left(1 + \frac{1}{\alpha_p^2}\right)\gamma} k_p^{-1}, \quad (3)$$

* pkmanwani@gmail.com

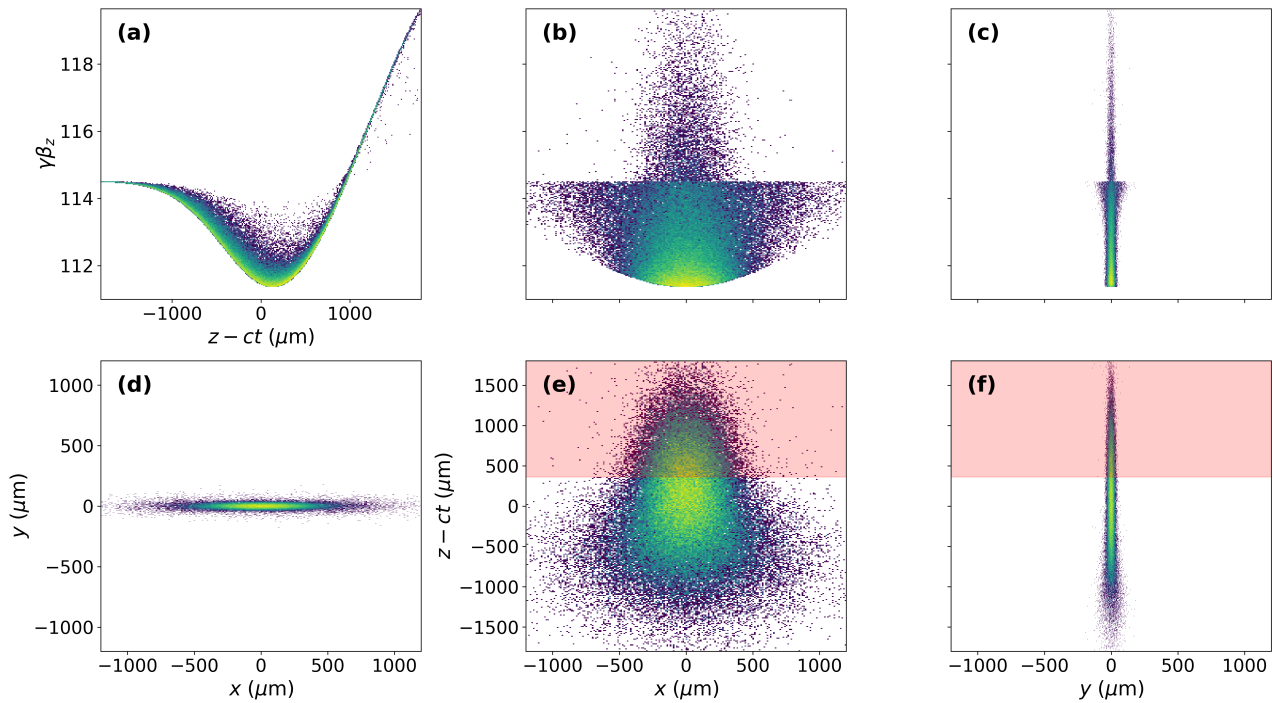


Figure 2: Phase space of the beam after the interaction. The longitudinal phase space is shown in (a). Panels (b) and (c) display transverse positions versus longitudinal momentum ($x-p_z$ and $y-p_z$ projections). The spatial distributions in the $x-y$, $x-z$, and $y-z$ planes are shown in panels (d), (e), and (f). The red shaded region in the lower panels highlights the tail portion of the beam being considered for further analysis.

where $k_p^{-1} = \sqrt{m_e \epsilon_0 c^2 / n_0 e^2}$ is the plasma skin depth which determines the length scale of the interaction, n_0 is the nominal plasma density, m_e is the electron mass and e is the electron charge.

Table 1: AWA Beam Parameters

Parameter	Value	Unit
Charge	2	nC
Energy	58	MeV
Horizontal emittance	200	μm rad
Vertical emittance	2	μm rad
Bunch length	600	μm
Plasma density, n_0	1×10^{14}	cm ⁻³
Plasma total length, L	4	cm
Plasma ramp, σ_p	0.25	cm

This creates the basis through which we can study the interaction of the particle beam available at the Argonne Wakefield Accelerator (AWA). The discharge-based capillary plasma source at UCLA can obtain a peak density of $10^{15} - 10^{16}$ cm⁻³, allowing for a range of operating points. This experiment involves creating a weak elliptical blowout using a flat beam driver, and the beam and expected operating plasma density are shown in Table 1. The ellipticity of the blowout can be obtained using the long beam limit where $k_p \sigma_z > 1$. This allows us to get the full vacuum-plasma transport and guides the beamline layout as is described in detail

in Ref. [9]. Based on this model of propagation, simulations are performed using QuickPIC [10], a 3-D quasi-static particle-in-cell (PIC) code, to study the beam-plasma interaction and the propagation of the flat beam. We assumed a ramped profile of the form of $n_0 e^{(-z^2/\sigma_p^2)}$ at the ends of the plasma. The blowout created by the flat beam at the midpoint of the plasma profile (2 cm into the profile), is shown in Fig. 1. For the transport study, we used Gaussian beams instead of flattop beams which yield slightly broader sheaths [11].

DIAGNOSTICS AND OBSERVABLES

We look at the beam phase space profiles after the interaction shown in Figure 2, as this would stipulate the diagnostic requirements for the experiment. The longitudinal phase space shows the deceleration and acceleration caused by the PWFA. This can be measured experimentally at AWA using a transverse deflecting cavity and a dipole spectrometer. The profiles showing the longitudinal momentum with the transverse position space reveal the coordinate dependence of the elliptical blowout and can be used as signatures of the ellipticity of the blowout. However, these measurements are challenging to obtain experimentally due to the necessity of accounting for external focusing and scattering effects. The lower panels show the beam projections in position space. To characterize the longitudinally varying focusing, an optical transition radiation (OTR) screen will be positioned at the exit of the capillary which will be viewed

with a streak camera [12]. The angular distribution of the beam at the capillary exit is inferred by measuring the transverse beam profiles on the OTR foil and two downstream screens placed at known distances along the beamline. By comparing the beam sizes and centroids across these three locations, the beam's divergence can be estimated from the spatial evolution of the transverse distribution. The back plane of the OTR foil will be used to prevent plasma light emission from masking the OTR signal. The three screens will also enable emittance characterization of the beam after the beam-plasma interaction. Betatron radiation generated during the flat-beam propagation could also serve as a possible diagnostic [13]. The simulated evolution of the beam spot size is shown in Figure 3. There is significant head erosion [14] as the interaction is in the weak blowout regime, where the front of the beam is not focused as it is outside the blowout cavity.

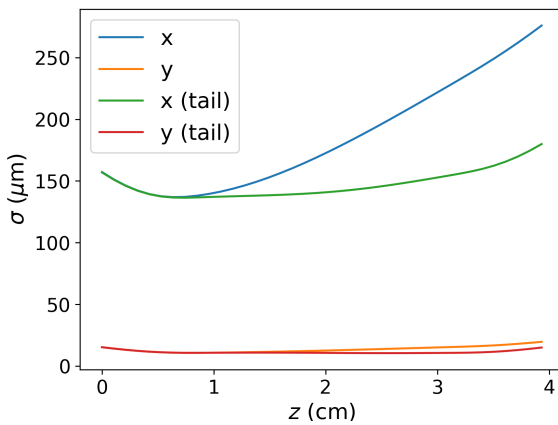


Figure 3: Beam spot size evolution during the beam-plasma interaction is shown. The tail of the beam stays matched while the head that is outside the blowout erodes.

CONCLUSION

This paper establishes the relationship between the flat beam PWFA theory and experiment, and utilizes the current progress made in understanding elliptical blowouts [7]. At the same time, it discusses the progress in the development of the discharge based capillary source and the beam transport at AWA, providing valuable insights on the measurable observables in the experiment. In parallel, work on gas–vacuum separation, as well as flat beam generation and characterization, is underway. This experiment would analyze the stable propagation of the matched flat beam driver in plasma, providing quantitative benchmarks against the simulations and theoretical models.

ACKNOWLEDGEMENTS

This work was performed with the support of the US Dept. of Energy under Contract No. DE-SC0017648 and DE0SC0009914.

REFERENCES

- [1] J. B. Rosenzweig *et al.*, “Acceleration and focusing of electrons in two-dimensional nonlinear plasma wake fields”, *Phys. Rev. A*, vol. 44, p. R6189–R6192, 1991. doi:10.1103/PhysRevA.44.R6189
- [2] W. Lu *et al.*, “A nonlinear theory for multidimensional relativistic plasma wave wakefields”, *Phys. Plasma*, vol. 13, no. 5, p. 056 709, 2006. doi:10.1063/1.2203364
- [3] A. Golovanov, I. Y. Kostyukov, A. Pukhov, and V. Malka, “Energy-conserving theory of the blowout regime of plasma wakefield”, *Phys. Rev. Lett.*, vol. 130, no. 10, p. 105 001, 2023. doi:10.1103/PhysRevLett.130.105001
- [4] P. Manwani, D. Chow, G. Andonian, J. Rosenzweig, N. Majernik, and Y. Kang, “Progress on the capillary plasma discharge source at UCLA”, in *Proc. IPAC’24*, Nashville, TN, USA, pp. 587–590, 2024. doi:10.18429/JACoW-IPAC2024-MOPR66
- [5] P. Manwani *et al.*, “Flat beam plasma wakefield accelerator”, in *2022 IEEE Adv. Accel. Concepts Workshop*, Long Island, NY, USA, Nov. 2022, pp. 1–5. doi:10.1109/AAC55212.2022.10822925
- [6] T. Xu *et al.*, “Demonstration of eigen-to-projected emittance mapping for an ellipsoidal electron bunch”, *Phys. Rev. Accel. Beams*, vol. 25, no. 4, p. 044 001, 2022. doi:10.1103/PhysRevAccelBeams.25.044001
- [7] P. Manwani, Y. Kang, J. Mann, B. Naranjo, G. Andonian, and J. B. Rosenzweig, “Analysis of the blowout plasma wakefields produced by drive beams with elliptical symmetry”, *Phys. Rev. Lett.*, in press. doi:10.1103/28c4-blhg
- [8] M. D. Litos, R. Ariniello, C. E. Doss, K. Hunt-Stone, and J. R. Cary, “Beam emittance preservation using gaussian density ramps in a beam-driven plasma wakefield accelerator”, *Phil. Trans. R. Soc. A*, vol. 377, no. 2151, 2019. doi:10.1098/rsta.2018.0181
- [9] P. Manwani, A. Ody, D. Chow, G. Andonian, J. Rosenzweig, and Y. Kang, “Flat beam transport for a PWFA experiment at AWA”, in *Proc. IPAC’24*, Nashville, TN, USA, pp. 580–582, 2024. doi:10.18429/JACoW-IPAC2024-MOPR64
- [10] C. Huang *et al.*, “Quickpic: A highly efficient particle-in-cell code for modeling wakefield acceleration in plasmas”, *J. Comput. Phys.*, vol. 217, no. 2, pp. 658–679, 2006. doi:<https://doi.org/10.1016/j.jcp.2006.01.039>
- [11] P. Manwani, Y. Kang, G. Andonian, J. Rosenzweig, and J. Mann, “Comparison of flat beam PWFA analytic model with PIC simulations”, in *Proc. IPAC’24*, Nashville, TN, USA, pp. 583–586, 2024. doi:10.18429/JACoW-IPAC2024-MOPR65
- [12] M. C. Thompson *et al.*, “Observations of low-aberration plasma lens focusing of relativistic electron beams at the underdense threshold”, *Physics of Plasmas*, vol. 17, no. 7, p. 073 105, 2010. doi:10.1063/1.3457924
- [13] M. Yadav *et al.*, “Radiation Diagnostics for AWA and FACET-II Flat Beams in Plasma”, in *Proc. IPAC’22*, Bangkok, Thailand, pp. 1791–1794, 2022. doi:10.18429/JACoW-IPAC2022-WEPOST042
- [14] S. Z. Li *et al.*, “Head erosion with emittance growth in pwfa”, *AIP Conf. Proc.*, vol. 1507, no. 1, pp. 582–587, 2012. doi:10.1063/1.4773762